Middle-East Journal of Scientific Research 16 (4): 536-547, 2013
ISSN 1990-9233

DOI: 10.5829/idosi.mejsr.2013.16.04.11717

Hybrid Adaptive Recurrent Neurofuzzy Based SVC Control for Damping Inter-Area Oscillations

Saima Ali, Shahid Qamar and Laiq Khan

Department of Electrical Engineering, COMSATS Institute of Information Technology, Abbottabad, Pakistan

Abstract: The study proposes a Static Var Compensator (SVC) design to improve the power system damping in the presence of some physical disturbances. An online hybrid Adaptive Recurrent Neuro Fuzzy (ARNF) control based on Gaussian membership function is presented in this paper to exaggerate the SVC to damp out oscillations. The proposed ARNF strategy is nonlinear and robust to meet the control objectives and to handle the uncertainties faster than traditional controllers. Due to the persistent nature of control it is vigorous to changed conditions and quickly restores the system's equilibrium. A back propagation algorithm is used to update the parameters of the proposed control and also to minimize the cost function. To evaluate the performance of proposed control strategy, a three machine test system is developed in MATLAB for different scenarios. The nonlinear simulation results were compared with Adaptive Proportional, Integral and Derivative (APID) and Adaptive Takagi, Sugeno and Kang (ATSK). These results show that the proposed ARNF control gives improved performance during both transient and steady-state regions and greatly increase the system damping.

Key words: Static Var Compensator · Adaptive Recurrent Neuro Fuzzy Control · Back propagation algorithm · MATLAB

INTRODUCTION

Several power system networks have experienced angular unsteadiness in the form of low frequency oscillations, mostly due to inadequate damping in the system. Two categories of low frequency oscillations are detected in the networks. One is the local area of oscillations linked with one or more generators in an area oscillating against the rest of the system. The other is the inter-area oscillations involving a group of generators on one side of the tie line oscillating against another group of generators on the other side. However, low frequency oscillations with the frequencies in the range of 0.2 to 2 Hz. As a result of these electromechanical modes of oscillations make the system vulnerable to cascading failures and a higher risk of instability of power system. Therefore, to maintain the stability of the whole system, it is very important to damp the electromechanical oscillations in a very short interval of time [1, 2]. To damp out these oscillations, many auxiliary stabilizing controls have been designed for devices such as power system stabilizers (PSS) [3, 4], Static Var Compensators (SVC) [5-9] and other Flexible AC Transmission System (FACTS) controllers [10-13].

The most popular type of FACTS controllers in terms of application is the SVC. SVC is functional for power oscillation damping, enhancement of stability and frequency stabilization [14]. By varying its reactance feature from inductive to capacitive, the SVC has the ability to control the power flow and improve the potential of power transfer in power systems. The SVC with supplementary control signal has the ability to enhance the stability and damping of power system oscillations in their voltage control loops [15]. In recent years, many researchers have presented schemes for regulating SVC stabilizers to improve the damping of electromechanical oscillations of power systems [16-18]. The fundamental drawback of these schemes is that the effect of load model parameters on tuning SVC stabilizer has not been taken into account. Almost all of SVC stabilizers have been tuned based on fixed load parameters. If the constraints of typical loads vary; consequently, the SVC stabilizers

Corresponding Author: Saima Ali, Department of Electrical Engineering, COMSATS Institute of Information Technology, Abbottabad, Pakistan.

tuned under set load parameters may become undesirable under other load parameters. Various techniques are presented for designing supplementary controllers in SVC. The conventional supplementary design, which offers a good dynamic performance under one scenario, may no longer yield the suitable results for the other scenario such as PI and PID control scheme [19, 20]. The amount of nonlinearity of a power system and a persistent change in the operating points make it very complex to attain a good stabilizer design, which gives acceptable performance over a broad range of operating conditions. To overcome this problem, some adaptive/self-tuning stabilizer designs have been recommended for PSS [21-23] and SVC [24]. A synchronized tuning of a PSS and a SVC controller based on Genetic Algorithm is suggested in [25]. In [26], a new strategy is represented to locate optimal position of SVCs to enhance power system stability. In order to improve power system stability, a new strategy based on wide area signals via SVC is proposed in [27]. In [28], a new hybrid technique is presented to simulate power systems equipped with SVC.

Recently, fuzzy logic and artificial neural network Controllers have appeared as an efficient tool to damp undesirable oscillations in power systems [29, 30]. In [31], a fuzzy logic control was proposed for SVC. Fuzzy logic approach is a burning tool for solving complex issues whose system performance is complex in nature. An attractive aspect of fuzzy logic control is its robustness to system parameters and shows flexibility when system's operating conditions varies [32, 33]. Fuzzy logic controllers (FLCs) are proficient of enduring vagueness and ambiguity to a greater degree [34]. Fuzzy logic strategy has been emphasized in power system issues of transient stability enhancement and damping of oscillations using FACTS devices [35-37]. However, the weaknesses of the fuzzy inference system were entirely based on the knowledge and experience of the human. Since both fuzzy logic and artificial neural network have their relative benefits, a powerful processing with both advantages can be achieved by merging them together. More recently, the use of adaptive neuro-fuzzy based power oscillation damping controllers has been suggested as an effective way. The adaptive neurofuzzy combines the advantages of fuzzy logic and neural network together. The learning ability of neural network is used to regulate the parameters of fuzzy logic in different scenarios to attain a better performance [38, 39]. However, a major drawback of the neurofuzzy system is that its application field is restricted to static problems due to its feed forward network composition. Processing sequential problems using the neurofuzzy system is inefficient. On other hand, ARNF structure is based on supervised learning, which is a dynamic mapping network and is more appropriate for dealing with dynamic systems than the neurofuzzy system [40-43].

This paper examines the design of an auxiliary hybrid Adaptive Recurrent based NeuroFuzzy (ARNF) controller to satisfy power oscillations by SVC. The ARNF is a recurrent multilayered connectionist network for determining the fuzzy inference system and can be developed from a set of fuzzy linguistic rules. The sequential relations entrenched in the ARNF are developed by summing feedback connections in the second layer of the fuzzy neural network. This adaptation provides the increase in memory elements of the ARNF and improves the basic ability of the fuzzy neural network to include sequential problems. Since a recurrent neuron has an inner feedback loop, it extracts the dynamic response of a system, thus the network model can be generalized and has the advantages of being dynamic and robust.

This ARNF has the self-learning ability of ANN with the linguistic expression function of recurrent fuzzy inference. By using a hybrid learning procedure, i.e. back-propagation, the parameters of membership functions and weights are optimized and can build an input-output mapping based on both human knowledge and stipulated input-output data pairs. The initial setting of membership functions for the fuzzy logic is done and to make it more flexible and nonlinear the antecedent part of fuzzy logic is made recurrent based on the dynamical behavior of SVC. Since, ARNF can be rated as an efficient and robust method for tuning the membership functions to reduce the measured output errors. An auxiliary ARNF based controller is developed to adapt the equivalent susceptance of the SVC during the transients to improve the stability of the power system. Subsequently, aiming to offer a fruitful examination, a comparative study is presented where the ARNF based controller is compared with conventional TSK and PID controller. Simulation results using MATLAB/Simulink authenticates the better damping of low frequency oscillations obtained with ARNF based controller. This paper is divided into VI sections. Sections II and III explains the SVC phasor modeling and multi machine power system for SVC installed. In the section IV proposed model ARNF system is presented. Finally, sections V and VI give the simulation results and conclusion of the work.

Svc Phasor Model and Control: An SVC is one of the renowned shunt connected FACTS controller which is used as a reactive compensator in power system. The SVC model used in this study is of TSC-TCR type. It generates reactive power (leading VARS) when its voltage is more than the system giving capacitive effect. However, it absorbs reactive power (lagging VARS) when its generated voltage is less as compared to system voltage and acts just like a reactor. The SVC phasor model and internal control is given as below:

SVC Phasor Model: The phasor model of SVC under balanced three phase AC system voltages can be represented as [44];

$$\bar{i}_{abc\_scv} = - B_{svc}\bar{e}_{abc\_svc} \quad (1)$$

$$\bar{i}_{abc\_scv} = \bar{i}_{TCR}(? _{svc}) + \bar{i}_{TSC} \quad (2)$$

where, $\bar{i}_{svc}$ defines the SVC injected current and $\bar{e}_{svc}$ gives the voltage generated by the SVC control.

$$\bar{i}_{TCR}(\psi_{svc}) = - \frac{V}{? L}\left(2-\frac{2\psi_{svc}}{p}+\frac{1}{p}\sin 2\psi_{svc}\right) \quad (3)$$

The SVC susceptance injected into the system is given by;

$$B_{svc} = B_{TCR}(\psi_{svc}) + B_{TSC} \quad (4)$$

here,

$$B_{TCR}(\psi_{svc}) = \frac{1}{? L}\left(2-\frac{2\psi_{svc}}{p}+\frac{1}{p}\sin 2\psi_{svc}\right) \quad (5)$$

The TSC-TCR type SVC usually consists of one TCR in parallel with 'n' TSC, so

$$B_{TSC} = nB_C \quad (6)$$

where $\psi_{svc} = \phi + \varphi,$ with 'ϕ' as a synchronizing angle and 'φ' is the firing angle and lies in the range of 90° to 180°. When $\psi_{svc}=90^o$, the SVC injects maximum susceptance while when $\psi_{svc}=180^o$, the SVC susceptance is zero. The reactive power injected by SVC is given by

$$Q_{inj\_svc} = - e_m{}^2 B_{svc} \quad (7)$$

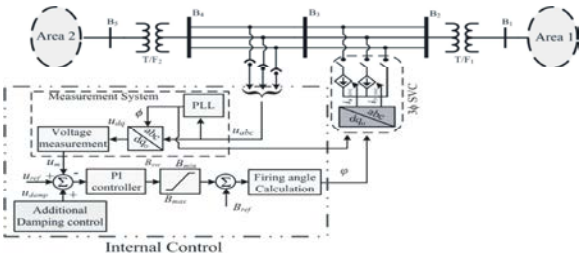

Fig. 1: SCV internal control connected to multi-machine power system

By using 'dq' reference frame, the current injected by SVC control can be written as follows;

$$\bar{i}_{dq\_svc} = \frac{2}{3}\begin{bmatrix}1 & a & a^2\end{bmatrix}\begin{bmatrix}\bar{i}_{a\_svc}\\ \bar{i}_{b\_svc}\\ \bar{i}_{c\_svc}\end{bmatrix}, \text{ where } a=e^{j\frac{2p}{3}} \quad (8)$$

SVC Internal Control: Fig. 3 shows the SVC with its internal main control connected to a multi-machine test system. The internal control consists of measurement unit, voltage regulator, synchronizing system and pulse generation module. The supplementary damping control is connected to the main control to provide additional damping to the system in consequent to its main task. The supplementary damping control used in this study is ARNF and is discussed in the proceeding section. The measurement module is used to provide the necessary inputs to other control blocks to perform their functions. Voltage and current is measured by using PT's and CT's. Output of measurement block is given as input to the voltage regulator. The voltage regulator compares this input voltage with reference to signal and generates the error signal which is sent as input to PI controller. The output of the controller is per unit susceptance which is generated to reduce the error signal to zero. Output of voltage regulator corresponds to the required reactive power output of compensator. Firing angle (φ) can be calculated by using susceptance to firing angle converter. The purpose of the phase locked loop (PLL) is to generate pulses (ϕ) that must be synchronized with the fundamental component of system voltage to minimize the harmonics.

Multi-Machine Power System with SVC Installed: The multi-machine power system dynamic model used in this study is given as follows [45];

$$\frac{dd}{dt} = \omega_{ref}\omega \tag{9}$$

$$M\frac{d\omega}{dt} = P_m - P_e - D\omega \tag{10}$$

$$T'_{qo}\frac{dE'_d}{dt} = \left(x_q - x'_q\right)I_q - E'_d \tag{11}$$

$$T'_{do}\frac{dE'_q}{dt} = E_{fd} - \left(x_d - x'_d\right)I_d - E'_d \tag{12}$$

$$T''_{qo}\frac{dE''_d}{dt} = \left(x_q - x''_q\right)I_q - E''_d \tag{13}$$

$$T''_{do}\frac{dE''_q}{dt} = E'_q - E''_q - \left(x'_d - x''_d\right)I_d \tag{14}$$

The stator algebraic equations with zero armature resistance are

$$\begin{bmatrix}\bar{U}_d\\ \bar{U}_q\end{bmatrix} = \begin{bmatrix}x''_q & 0\\ 0 & x''_d\end{bmatrix}\begin{bmatrix}\bar{I}_q\\ \bar{I}_d\end{bmatrix} + \begin{bmatrix}E''_d\\ E''_q\end{bmatrix} \tag{15}$$

The terminal voltage of the generators in machine coordinates can be expressed as

$$\bar{U}_G = E''_d + x''_q I_q + j\left(E''_q - x''_d I_d\right) \tag{16}$$

The network model before installation of SVC, between bus bars 2 and 3 is given as;

$$\begin{bmatrix}0\\0\\0\\0\\\bar{i}_G\end{bmatrix} = \begin{bmatrix}\bar{Y}_{11} & \bar{Y}_{12} & \bar{Y}_{13} & \bar{Y}_{1G}\\ \bar{Y}_{21} & \bar{Y}_{22} & \bar{Y}_{23} & \bar{Y}_{2G}\\ \bar{Y}_{31} & \bar{Y}_{32} & \bar{Y}_{33} & \bar{Y}_{3G}\\ \bar{Y}_{41} & \bar{Y}_{42} & \bar{Y}_{43} & \bar{Y}_{4G}\\ \bar{Y}_{G1} & \bar{Y}_{G2} & \bar{Y}_{G3} & \bar{Y}_{GG}\end{bmatrix}\begin{bmatrix}\bar{U}_1\\ \bar{U}_2\\ \bar{U}3\\ \bar{U}_K\\ \bar{U}_G\end{bmatrix} \tag{17}$$

After installation of SVC into the network, the network model can be written as

$$\begin{bmatrix}\bar{Y}_{11} & 0 & 0 & \bar{Y}_{1G}\\ 0 & \bar{Y}'_{22} & 0 & \bar{Y}_{2G}\\ 0 & 0 & \bar{Y}'_{33} & \bar{Y}_{3G}\\ \bar{Y}_{G1} & \bar{Y}'_{G2} & \bar{Y}_{G3} & \bar{Y}_{GG}\end{bmatrix}\begin{bmatrix}\bar{U}_1\\ \bar{U}_2\\ \bar{U}_3\\ \bar{U}_G\end{bmatrix} = \begin{bmatrix}-\bar{i}_{1K}\\ -\bar{i}_{2K}\\ -\bar{i}_{3K}\\ \bar{i}_G\end{bmatrix} \tag{18}$$

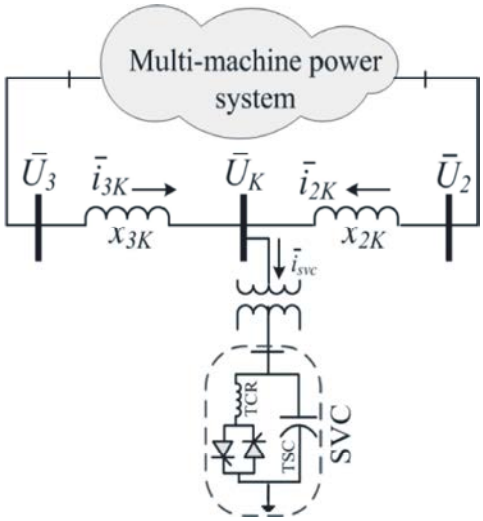

Fig. 2: SVC connected between bus bars 2 and 3

The output voltage of SVC in phasor form is given by;

$$\bar{e}_{svc} = e_m \angle ?_{svc} \tag{19}$$

From Fig. 2, the voltage difference across the coupling transformer is

$$\bar{U}_K = jx_c\bar{i}_{svc} + \bar{e}_{svc} \tag{20}$$

where,

$$\bar{i}_{svc} = \bar{i}_{2K} + \bar{i}_{3K} \tag{21}$$

The voltage at the bus bars 2 and 3 can be written as

$$\begin{bmatrix}\bar{U}_2\\ \bar{U}_3\end{bmatrix} = \begin{bmatrix}jx_{2K} & 0\\ 0 & jx_{3K}\end{bmatrix}\begin{bmatrix}\bar{i}_{2K}\\ \bar{i}_{3K}\end{bmatrix} + \begin{bmatrix}1\\1\end{bmatrix}\bar{U}_K \tag{22}$$

Putting value of $\bar{U}_K$ from (20) in (22),

$$\begin{bmatrix}\bar{U}_2\\ \bar{U}_3\end{bmatrix} = \begin{bmatrix}j\left(x_{2K}+x_c\right) & jx_c\\ jx_c & j\left(x_{3K}+x_c\right)\end{bmatrix}\begin{bmatrix}\bar{i}_{2K}\\ \bar{i}_{3K}\end{bmatrix} + \begin{bmatrix}1\\1\end{bmatrix}\bar{e}_{svc} \tag{23}$$

$$\begin{bmatrix}\bar{i}_{2K}\\ \bar{i}_{3K}\end{bmatrix} = \frac{1}{X}\begin{bmatrix}j\left(x_{2K}+x_c\right) & -jx_c\\ -jx_c & j\left(x_{3K}+x_c\right)\end{bmatrix}\begin{bmatrix}\bar{U}_2 - \bar{e}_{svc}\\ \bar{U}_3 - \bar{e}_{svc}\end{bmatrix} \tag{24}$$

where,

$$X = x_c^2 - \left(x_{2K}+x_c\right)\left(x_{3K}+x_c\right) \tag{25}$$

The generator current is then given as,

$$\bar{i}_G = \left(\bar{Y}_{GG} - \begin{bmatrix} \bar{Y}_{G2} & \bar{Y}_{G3} \end{bmatrix} \bar{Y}_{U_{23}}^{-1} \begin{bmatrix} \bar{Y}_{2G} \\ \bar{Y}_{3G} \end{bmatrix} \right) \bar{U}_G + \begin{bmatrix} \bar{Y}_{G2} & \bar{Y}_{G3} \end{bmatrix} \bar{Y}_{U_{23}}^{-1} \begin{bmatrix} j\frac{x_{2K}}{X} \\ j\frac{x_{3K}}{X} \end{bmatrix} \bar{e}_{svc} \quad (26)$$

where,

$$\bar{Y}_{U_{23}}^{-1} = \begin{bmatrix} \bar{Y}'_{22} + \frac{j(x_{2K}+x_c)}{X} & \frac{-jx_c}{X} \\ \frac{-jx_c}{X} & \bar{Y}'_{33} + \frac{j(x_{3K}+x_c)}{X} \end{bmatrix}$$

Proposed Adaptive Recurrent Neurofuzzy Control: In this section, the proposed hybrid Adaptive Recurrent NeuroFuzzy (ARNF) is presented to illustrate that the ARNF is a system simplified from the neurofuzzy system. The key features of the ARNF are that, it has dynamic mapping potential, temporal memory, universal estimation and the fuzzy inference system.

This section presents a fuzzy inference system implemented by using a multilayer recurrent neural network, called an ARNF. A schematic diagram of the proposed hybrid ARNF structure is shown in Fig. 3, which is organized into *n*input variables, m- nodes for each input variable, p' output nodes, m×n and rule nodes. This ARNF system thus consists of six layers. Layer I accepts input variables. Its nodes represent input linguistic variables. Layer II is used to estimate Gaussian membership function. The Gaussian function is adopted as the membership function. Nodes in this layer characterize the terms of the particular linguistic variables. Nodes at layer III signify fuzzy rules. Layer III forms the fuzzy rule base. Links before layer III represent the prerequisites of the rules and the links after layer III characterize the consequences of the rule nodes. Layer IV represents the weights w_{ip} of neural systems and layer V and IV represent the defuzzification of the neurofuzzy system.

ARNF Layered Structure: A fuzzy logic system normally accumulates its data in the shape of a fuzzy algorithm [46], which consists of a fuzzy linguistic rules relating to the input and output of the network. Then the ´min´ rule has the form:

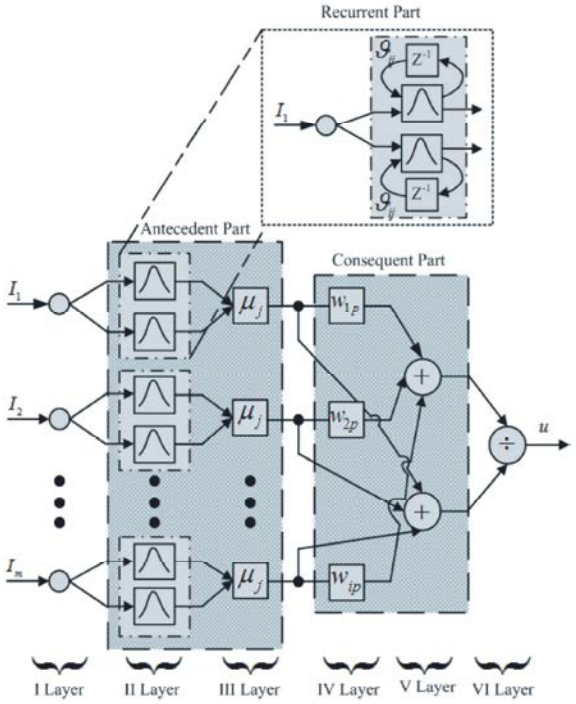

Fig. 3: ARNF Layered Structure

$$\begin{aligned} &R_1\text{: If } I_{11} \text{ is } A_{11} \text{ and } I_{12} \text{ is } A_{12} \text{ and } \ldots I_{1n} \text{ is } A_{1n} \text{ Then } \hat{y}_1 \text{ is } B_1 \\ &R_2\text{: If } I_{21} \text{ is } A_{21} \text{ and } I_{22} \text{ is } A_{22} \text{ and } \ldots I_{2n} \text{ is } A_{2n} \text{ Then } \hat{y}_2 \text{ is } B_1 \\ &\quad\vdots \qquad\qquad\qquad\qquad\qquad\qquad \vdots \\ &R_m\text{: If } I_{m1} \text{ is } A_{m1} \text{ and } I_{m2} \text{ is } A_{m2} \text{ and } \ldots I_{mn} \text{ is } A_{mn} \text{ Then } \hat{y}_m \text{ is } B_m \end{aligned} \quad (27)$$

Where, $I_1, I_2, \ldots I_n$ and $\hat{y}_1, \hat{y}_2, \ldots, \hat{y}_m$ are the inputs-outputs variables and A_{ij} shows the Gaussian membership functions of i^{th} input and j^{th} rule. The output of the system can be expressed as:

$$u = \frac{\sum_{i=1}^{m} \mu_{ij} w_{ip}}{\sum_{i=1}^{m} \mu_{ij}} \quad (28)$$

The structure for the ARNF network is depicted in Fig. 3. It comprises of six layers:

Layer I: This layer is the input layer, i.e. introduces the inputs $I_1, I_2, \ldots I_n$. This layer accepts the input values and transmits it to the next layer.

Layer II: In this layer the fuzzification process is performed and neurons represent fuzzy sets used in the antecedents' p art of the linguistic fuzzy rules. The

outputs of this layer are the values of the membership functions, i.e. $\mu_{ij}(k)$. The membership of i^{th} input variable to j^{th} fuzzy set is defined by Gaussian membership function and be represented as.

$$\eta_{ij}(k) = e^{-\frac{(I_i(k)-g_{ij})^2}{s_{ij}^2}} \quad (29)$$

and

$$I_i(k) = O^1(k)+O^2(k); \quad k=1, 2, ..., n$$

where,

$$O^2(k) = \eta_{ij}(k-1).\vartheta_{ij}(k) \quad (30)$$

So $\eta_{ij}(k)$ can be written as

$$\eta_{ij}(k) = e^{-\left(\frac{O^1(k)+\eta_{ij}(k-1).\vartheta_{ij}(k)-g_{ij})}{s_{ij}}\right)^2} \quad (31)$$

where $'g_{ij}'$ is the mean and $'s_{ij}'$ is the variance of the membership function. $O^1(K)$ is the input to the first layer, $\eta_{ij}(k-1)$ is the previous value of membership function and $\vartheta_{ij}(k)$ represents the linkage weight to the feedback unit. It is clear that the input of this layer contains the memory terms $\eta_{ij}(k-1)$, which store the previous information of the network. This is the clear difference between the neurofuzzy and recurrent neurofuzzy system.

Layer III: This layer is the fuzzy inference layer. In this layer each node represents a fuzzy rule. In order to compute the firing strength of each rule and *min* operation is used to estimate the output value of the layer. i.e.

$$\mu_{ij}(k) = \prod_i \eta_{ij}(k) \quad (32)$$

Where is the Π operation, $\eta_{ij}(k)$ are the degrees of the membership function of the layer II and $\mu_{ij}(k)$ are the input values for the next layer.

Layer IV: This layer represents the hidden weights w_{ip} of the ARNF system.

Layer V and VI: These layer operates the defuzzification process, i.e.

$$u = \frac{\sum_{i=1}^{m}\mu_{ij}w_{ip}}{\sum_{i=1}^{m}\mu_{ij}} \quad (33)$$

where, $'u'$ is the output for the entire network. The training of the network starts after estimating the output value of the ARNF system and w_{ip} are the weights between the neurons of III and IV layers and $p = 1, 2, ..., n;'n'$ is the number of classes.

Learning of Update Parameters: The ARNF learning process is to minimize the error input and output values by adjusting network parameters. The gradient descent method is used to adjust the values of weights $'w_{ip}'$ and mean $'m_{ij}'$ and variance $'s_{ij}'$ of the membership function ARNF. To minimize the error between the actual output value of the system and the desired value, a gradient descent method is used and can be can be expressed as;

$$E(k) = \frac{1}{2}\left(y_d(k) - y(k)\right)^2 \quad (34)$$

Where $'y_d'$ and $'y'$ are the actual and desired output of the system. By using the back propagation learning algorithm, the updating parameters of the ARNF is fine-tuned such that the cost function defined in (34) is less than a desired value. By recursive functions of the chain rule, the error expression for each layer is first calculated and then the parameters in the corresponding layers are adjusted. The famous back propagation algorithm for w_{ip}, m_{ij}, s_{ij} and ϑ_{ij} may be expressed as

$$w_{ip}(k+1) = w_{ip}(k) - \gamma\frac{\partial E}{\partial w_{ip}} \quad (35)$$

$$g_{ij}(k+1) = m_{ij}(k) - \gamma\frac{\partial E}{\partial g_{ij}} \quad (36)$$

$$s_{ij}(k+1) = s_{ij}(k) - \gamma\frac{\partial E}{\partial s_{ij}} \quad (37)$$

$$\vartheta_{ij}(k+1) = \vartheta_{ij}(k) - \gamma\frac{\partial E}{\partial \vartheta_{ij}} \quad (38)$$

Where, γ shows the learning rate. The chain rule for the w_{ip}, m_{ij} σ_{ij}, and ∂_{ij} can be represented as;

$$\frac{\partial E}{\partial w_{ip}} = \frac{\partial E}{\partial y}.\frac{\partial y}{\partial u}.\frac{\partial u}{\partial w_{ip}} \quad (39)$$

$$\frac{\partial E}{\partial g_{ij}}=\frac{\partial E}{\partial y}.\frac{\partial y}{\partial u}.\frac{\partial u}{\partial \mu_{ij}}.\frac{\partial \mu_{ij}}{\partial g_{ij}} \quad (40)$$

$$\frac{\partial E}{\partial \sigma_{ij}}=\frac{\partial E}{\partial y}.\frac{\partial y}{\partial u}.\frac{\partial u}{\partial \mu_{ij}}.\frac{\partial \mu_{ij}}{\partial \sigma_{ij}} \quad (41)$$

$$\frac{\partial E}{\partial \vartheta_{ij}}=\frac{\partial E}{\partial y}.\frac{\partial y}{\partial u}.\frac{\partial u}{\partial \mu_{ij}}.\frac{\partial \mu_{ij}}{\partial \vartheta_{ij}} \quad (42)$$

By taking the derivative of the above equations, it gives

$$\frac{\partial E}{\partial w_{ip}}=-(y_d-y).\kappa.\frac{\mu_i}{\sum_{i=1}^{m}\mu_i} \quad (43)$$

$$\frac{\partial E(k)}{\partial g_{ij}}=-(y_d(k)-y(k)).\kappa.\frac{w_{ip}-u}{\sum_{i=1}^{m}\mu_i}.\mu_j(k)\,2\left(\frac{O^1(k)+?_j(k-1).\vartheta_{ij}(k)-g_{ij}}{s_{ij}^2}\right) \quad (44)$$

$$\frac{\partial E(k)}{\partial s_{ij}}=-(y_d(k)-y(k)).\kappa.\frac{w_{ip}-u}{\sum_{i=1}^{m}\mu_i}.\mu_j(k)\,2\left(\frac{O^1(k)+?_j(k-1).\vartheta_{ij}(k)-g_{ij}}{s_{ij}^3}\right) \quad (45)$$

$$\frac{\partial E(k)}{\partial \vartheta_{ij}}=-(y_d(k)-y(k)).\kappa.\frac{w_{ip}-u}{\sum_{i=1}^{m}\mu_i}.\mu_j(k)\,2?_{ij}(k-1)\left(\frac{O^1(k)+?_j(k-1).\vartheta_{ik}(k)-g_{ij}}{s_{ij}^2}\right) \quad (46)$$

Where, the quantity $\frac{\partial y}{\partial u}$ is approximated by a constant κ [47]. These above equations give the required change in update parameters of ARNF network.

RESULT AND DISCUSSION

To justify the performance of proposed supplementary control strategy for SVC, the nonlinear simulations were carried out in a multi-machine power system. The system is divided into two areas having three machines, four loads and 6 bus bars. The areas are interconnected by two tie-lines with the help of step-up transformers. Generator-1 (G_1) is placed in area 1 while Generator-2 (G_2) and Generator-3 (G_3) are in area 2 as shown in Fig. 4. To damp the inter-area power oscillations, the SVC based power system model is implemented in the MATLAB/Simulink toolbox. The SVC is connected near bus 3 at the mid of the transmission line L_1. The transmission lines, loads and machines parameters and are provided in Table 1.

Table 1: Multi-machine power system parameters and data

Type of Data	Parameters
Generators	S_1= 4200MVA, S_2= S_3= 2100 MVA, H = 3.7 sec, v =13.8 kV, f = 60 Hz, R_s= 2.8544e-1, X_d= 1.305, X'_d= 0.296, X''_d= 0.252, X_q= 0.474, X'_q= 0.243, X''_q= 0.18, T_d= 0.101 sec, T_{qo}= 0.1 sec, $T_d^{'}$= 0.053 sec, P_{e1}= 0.9748, P_{e2}= 0.6094, P_{e3}= 0.419
Loads	Load 1= 7500 MW+1500 MVAR, Load 2=Load 3 = 25 MW, Load 4 = 250 MW
Transformers	S_{T1}= 4200 MVA, S_{T2}= S_{T3}= 2100 MVA, 13.8/500 kV, 60 Hz, R_1= R_2= 0.002, L_1= 0, L_2= 0.12, R_m= 500, L_m= 500
Transmission lines	3-phase, L_1=350 km, L_2=50 km, L_3=100 km, R_1=0.0254 O/*km*, R_o= 0.3864 O/km, L_1= 0.9337e^{-3} H/km, L_0= 4.126e^{-3} H/km, C_1=12.74e^{-9} F/km, C_o= 7.751e^{-9} F/km

The power flow analysis is performed on the test system by taking G_1 as a swing bus, G_2 and G_3 as a PV generator buses. The initial operating conditions for G_1 are 4095 MW, 1794 MVAR, for G_2 and G_3 are 1279 MW, 321 MVAR and 871 MW, 177 MVAR, respectively. The simulation results of proposed SVC-ARNF control are compared with that of SVC-ATSK control and SVC-APID.

Table 2: Settling Time Performance Improvement

		Performance improvement (%) for ARNF Control			
		δ_{21}		δ_{31}	
	Rotor angle Deviation	ATSK Control	APID Control	ATSK Control	APID Control
Case 1	Single line to ground fault	40.6	52.66	36.6	54.34
	Multiple small perturbance	25	34.5	22.7	33
Case 2	Three phase to ground fault	38	49	33.7	47.12
	Sudden load rejection	36.5	53.7	35.79	51.49

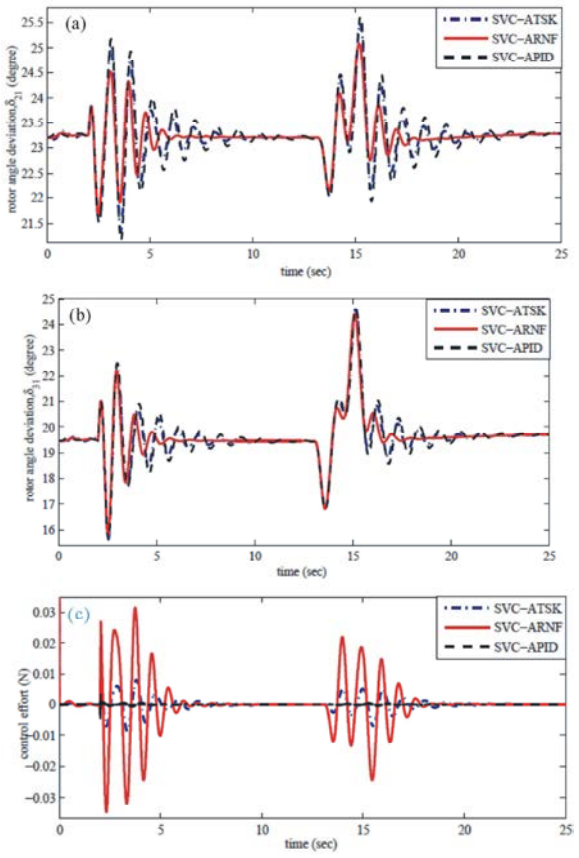

(a): Rotor angle deviation (δ_{21})
(b): Rotor angle deviation (δ_{31})
(c): Control effort

Fig. 5: Case 1 Single phase to ground fault

To guarantee the efficiency and robustness of the proposed ARNF control approach, different types of large and small perturbance are added to the power system during simulations. They are categorized into two cases as discussed in the subsection.

Case 1: Small Perturbance

Single Line to Ground Fault: To examine the effectiveness of the proposed ARNF control strategy, a 3 cycle single phase to ground fault is applied on transmission line L_3 at t= 2 sec near bus 6. The fault is self cleared at t=2.05 sec. Fig. 5(a) and Fig. 5(b) shows the inter-area rotor angle deviation of the perturbed system. The post fault system response in steady state region is oscillatory with SVC-APID and SVC-ATSK control whereas less oscillation can be observed with SVC-ARNF control as shown in Figure. Fig. 5(a) reveals that in the first swing, the overshoot of the system is decreased very much with SVC-ARNF which shows its improved performance during the transient state. The settling time of proposed control is also reduced very much as compared to other control strategies which is summarize in Table 2.

The control effort provided by the respective control schemes is shown in Fig. 5(c). It can be seen from result that when the fault occurs in the system, then the SVC-ARNF increases its control effort to bring the system to a stable equilibrium point and to damp the oscilations quickly.

Multiple Small Perturbances: in this case two different types of physical perturbances are added to the multi-machine power system. In the first case, a 3 cycle self cleared single phase to ground fault is applied at t=2 sec and in the second case, a step increase in the mechanical power of G_3 is added to the system at t=13 sec. The system remains in this faulty condition for about 1.5 sec. In case SVC-APID and SVC-ATSK control strategies, the damping is improved but still oscillatory behavior can be seen in steady state region. With the proposed SVC-ARNF, the rotor angle oscillations are damped out fully and the system regain its equilibrium state after being subject to this physical perturbance as shown in Fig. 6 (a) and Fig. 6 (b). The force applied by

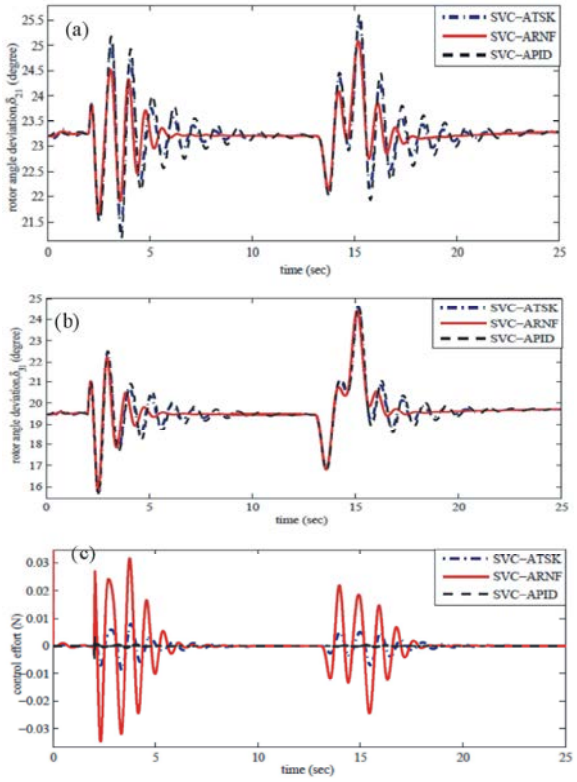

(a): Rotor angle deviation (δ_{21})
(b): Rotor angle deviation (δ_{31})
(c): Control effort

Fig. 6: Case 1 multiple small faults

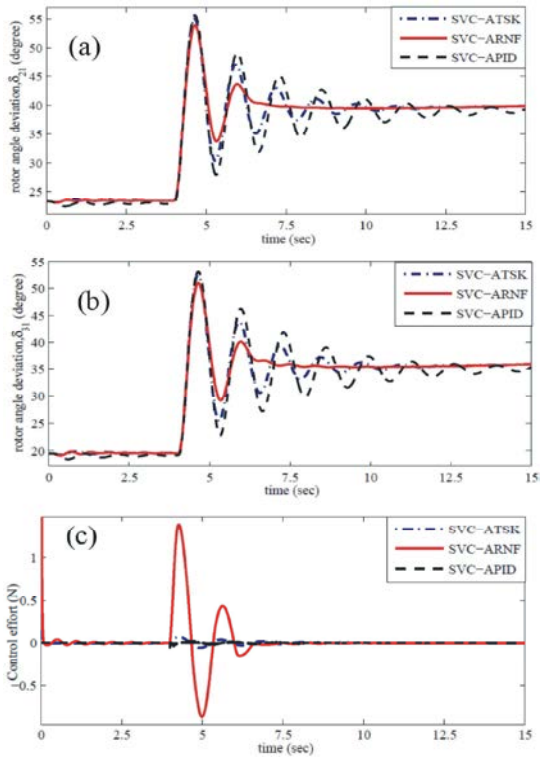

(a): Rotor angle deviation (δ_{21})
(b): Rotor angle deviation (δ_{31})
(c): Control effort

Fig. 7: Case 2 Three phase to ground fault

each control to damp the mechanical oscillations is shown in Fig. 6(c). The numerical values of improved overshoot and settling time of the SCV-ARNF can be seen from Table 2.

Case 2: Large Perturbance

Three Phase to Ground Fault: To further investigate the robust efficiency of the proposed SVC-ARNF control a 3 cycle, three phase to ground fault at t=4 sec is applied on line L_{12}. The fault is cleared by permanently removing the line L_{12}. Due to this severe perturbance, the system response is drifting very much and the rotors of the generators starts oscillating among each other. As a result of these mechanical oscillations, the system becomes unstable. Fig. 7(a) and Fig. 7(b) shows the rotor angle deviation δ_{21} and δ_{31} respectively. These results show that in case of SVC-ARNF, the post fault oscillations are completely damped out whereas oscillations can be seen in case of both SVC-ATSK and SVC-APID. The transient and steady state response of proposed SVC-ARNF is better than the other control strategies. The simulations also reveal that due to line removal, the system operating point is changed and moves to a new steady state condition. This mean that the SVC-ARNF shows robustness to keep the system on an optimal operating conditions. The overshoot and settling time of proposed SVC-ARNF are reduced very much as compered to other control schemes as shown in Table 2. The effort provided by each control to regain the system to new stable equilibrium state is shown in Fig. 7(c).

Sudden Load Rejection: In this case, the performance of the proposed control is analyzed by suddenly dis-connecting the 250 MW load (Load 4) at t=2 sec for 9 cycles. The fault is self cleared by re-connecting the load at t=2.15 sec. Due to this large load rejection transients are produced in the system and its overshoot increases significantly in the first swing as shown in Fig. 8(a) and

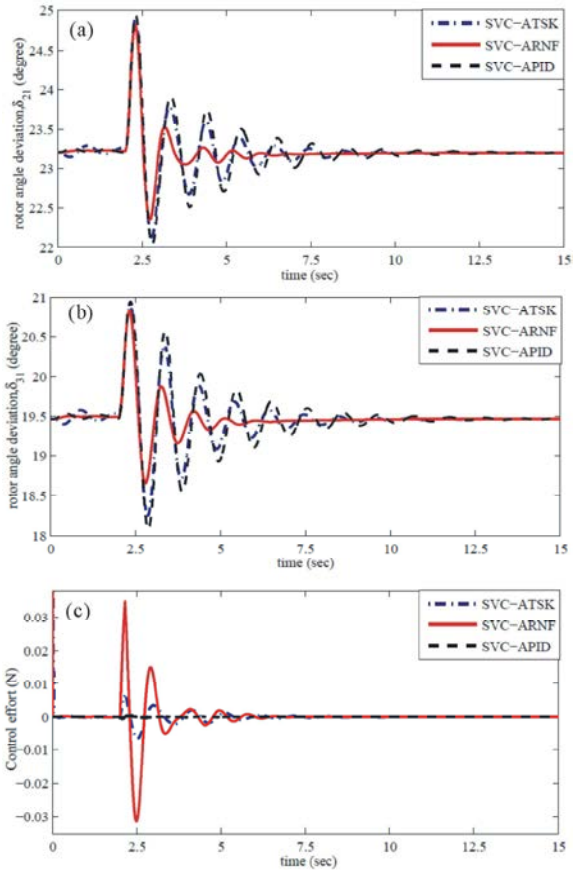

(a): Rotor angle deviation (δ_{21})
(b): Rotor angle deviation (δ_{31})
(c): Control effort

Fig. 8: Case 2 Sudden load rejection

Fig. 8(b). It can be observed from the results that with SVC-ARNF control, the overshoot in the second swing is reduced very much and also it brings the system back to its original steady state very quickly as compared to both SVC-ATSK and SVC-APID control. The improved response of proposed SVC-ARNF during transient and steady state regions shows its effectiveness and superiority over the other control schemes. Fig. 8(c) shows the control effort given by each adaptive control to damp the inter-area oscillations.

CONCLUSION

In this study ARNF control strategy has been effectively implemented as a supplementary control for SVC to damp the power system oscillations. The ARNF control parameters are tuned online using back propagation learning algorithm. A three machine power system along with SVC connected in the mid way has been considered as a test system in MATLAB/SIMULINK. To evaluate the proposed control performance various kinds of physical disturbances are added to the simulated system and then respective results are compared with APID control and ATSK. The simulation results show that the designed SVC-ARNF control has the ability to guarantee the system damping under the perturbed conditions. The proposed control strategies also increase the convergence and robustness of the system. Also, the computational ability of the proposed ARNF technique is better than the APID and ATSK techniques.

REFERENCE

1. Kundur, P., 1994. Power system stability and control. Prentice-Hall, New York, U.S.A.
2. Anderson, P.M. and A.A. Fouad, 1997. Power System Control and Stability. IEEE Press.
3. Demello, F.P. and C. Concordia, 1969. Concepts of Synchronous Machine Stability as Affected by Excitation Control. IEEE Transactions on Power Apparatus and Systems, PAS, 88(4): 316-329.
4. Kundur, P., M. Klein, G.J. Rogers and M.S. Sywno, 1989. Application of Power System Stabilizer for Enhancement of Overall System Stability. IEEE Transactions on Power System, 4(2): 6 14- 626.
5. Angquist, L., B. Lundin and J. Samuelsson, 1993. Power Oscillation Dampmg Using Controlled Reactive Power Compensation - A Comparison Between Series and Shunt Approach. IEEE Transactions on Power System, 8(2): 687-700.
6. Noroozian, M. and G. Anderson, 1995. Damping of Inter-Area and Local Modes by use of Controllable Components. IEEE Transactions on Power Delivery, 10(4): 2007-2012.
7. Aboul-Ela, M.E., A.A. Sallam and J.D. Mccalley, 1996. Damping Controller Design for Power System Oscillations Using Global Signals. IEEE Transactions on Power Delivery, 11(2): 767-773.
8. Rahim, A.H.M.A. and S.G.A. Nassimi, 1996. Synchronous Generator Damping Enhancement through Coordinated Control of Exciter and SVC. IEE Proceedings on Generation, Transmission and Distribution, 143(2): 211-218.

9. Wang, H.F. and F.J. Swift, 1996. Capability of the Static Var Compensator in Damping Power System Oscillations. IEE Proceedings on Generation, Transmission and Distribution, 143(4): 353-358.
10. Gronquist, J.F., W.A. Sethares, F.L. Alvxrado and R.H. Lasseter, 1995. Power Oscillation Damping Control Strategies for FACTS Devices using Locally Measurable Quantities. IEEE Transactions on Power Systems, 10(3): 1598-1605.
11. Pourbeik, P. and M.J. Gibbard, 1996. Damping and Synchronizing Torques Induced on Generators by Facts Stabilizers in Multimachine Power System. IEEE Transactions on Power Systems, 11(4): 1920-1925.
12. Taranto, G.N., J.K. Shiau, J.H. Chow and H.A. Othnian, 1997. Robust Decentralized Design for Multiple FACTS Damping Controllers. IEE Proceedings on Generation, Transmission and Distribution, 144(1): 61-67.
13. Wang, H.F. and F.J. Swllt, 1997. Unified Model for the Analysis of FACTS Devices in Damping Power Oscillation Part I: Single Machine Infinite Bus Power Systems. IEEE Transactions on Power Delivery, Pid, 12(2): 941-946.
14. Rai, D., S. Faried, G. Ramakrishna and A. Edris, 2010. Hybrid Series Compensation Scheme Capable of Damping Subsynchronous Resonance. IEE Proceedings on Generation, Transmission and Distribution, 4(3): 456-466.
15. Milanovic, J.V. and I.A. Hiskens, 1998. Damping Enhancement by Robust Tuning of SVC Controllers in the Presence of Load Parameters Uncertainty. IEEE Transaction on Power Systems, 13(4): 1298-1303.
16. Chang, C.S., Q.Z Yu, A.C. Liew and S. Elangovan, 1997. Genetic algorithm tuning of fuzzy SVC for damping power system inter-area oscillations. In the Fourth International Conference on Advances in Power System Control, Operation and Management (APSCOM-97), pp: 509-514.
17. Ellithy, K.A. and S.M. Al-Alawi, 1996. Tuning a Static Var Compensator Controller over a Wide Range of Load Models Using an Artificial Neural Network. Electric Power Systems Research, 38: 97-104.
18. Milanovic, J.V., 1997. Tuning of SVC Stabilizer to Compensate the Influence of Voltage Dependent Loads. The 36th IEEE Conference, 3: 2553-2558.
19. Chang, Y. and Z. Xu, 2007. A Novel SVC Supplementary Controllers Based on Wide Area Signals. Electric Power System Research, 77: 1569-1574.
20. Rahman, H., R. I. Sheikh and H. Rashid, 2013. Stability Improvement of Power System by using PI and PD Controller. Computer Technology and Application, 4: 111-118.
21. Hsu, Y.Y. and C.R. Chen, 1991. Turing of Power System Stabilizers Using an Artificial Neural Network. IEEE Transactions on Energy Conversions, 6(4): 612-617.
22. Zhang, Y., C.P. Chen, O.P. Malik and G.S. Hope, 1993. An Artificial Neural Network Based Adaptive Power System Stabilizer. IEEE Transactions on Energy Conversion, 8(1): 11-77.
23. Takanto, G.N., J.H. Chow and H.A. Othman, 1995. Robust Redesign of Power System Damping Controllers. IEEE Transactions on Control Systems Technology, 3(3): 290-298.
24. Zhao, Q. and J. Jiang, 1998. Robust Controller Design for Improving Power System Damping. IEEE Transactions on Power System, 10(4): 1921-1932.
25. Panda, S., N. Patidar and R. Singh, 2009. Simultaneous Tuning of SVC and Power System Stabilizer Employing Real Coded Genetic Algorithm. International Journal of Electrical Power and Energy Systems Engineering, 4(4): 240-247.
26. Haque, M., 2007. Best Location of SVC to Improve First Swing Stability of a Power System. International Journal of Electric Power System Research, 77(10): 1402-1409.
27. Chang, Y. and Z. Xu, 2007. A Novel SVC Supplementary Controller Based on Wide Area Signals. International Journal of Electric Power System Research, 77(12): 1569-1574.
28. Zhijun, E., D. Fang, K. Chan and S. Yuan, 2009. Hybrid Simulation of Power Systems with SVC Dynamic Phasor Model. International Journal of Electric Power System Research, 31(5): 175-178.
29. Karpagam, N. and D. Devaraj, 2009. Fuzzy logic control of Static Var Compensator for Power System Damping. International Journal of Electrical Power and Energy Systems, 2(2): 105-111.
30. Park, Y. M., M.S. Choi and K.Y. Lee, 1996. A Neural Network-Based Power System Stabilizer using Power Flow Characteristics. IEEE Transactions on Energy Conversion, 11(2): 435-441.
31. Gu, Q., A. Pandey and S.K. Starrett, 2003. Fuzzy Logic Control Schemes for Static VAR Compensator to Control System Damping using Global Signal. Electric Power System Research, 67: 115-122.

32. Lu, J., M.H. Nehrir and D.A. Pierre, 2004. A Fuzzy Logic-Based Adaptive Damping Controller for Static VAR Compensator. Electric Power System Research, 68: 113-118.
33. Phorang, K., M. Leelajindakraireak and Y. Mizutani, 2002. Damping Improvement of Oscillation in Power System by Fuzzy Logic Based SVC Stabilizer. In Asia Pacific Conference 2002, IEEE/PES Transmission and Distribution Conference and Exhibition, 3: 1542-1547.
34. Fang, D.Z., Y. Xiao Dong, T.S. Chung and K.P. Wong, 2004. Adaptive Fuzzy-Logic SVC Damping Controller using Strategy of Oscillation Energy Descent. IEEE Transactions on Power System, 9(3): 1414-1421.
35. Lo, K.L. and L. Khan, 2000. Fuzzy Logic Based SVC for Power System Transient Stability Enhancement. In the International Conference on Electric Utility Deregulation and Restructuring and Power Technologies (DRPT 2000), pp: 453-458.
36. Dash, P.K. and S. Mishra, 2003. Damping of Multimodal Power System Oscillations by FACTS Devices using Non Linear Takagi-Sugeno Fuzzy Controller. Electric Power System Research, 25: 481-490.
37. Radman, G. and R.S. Raje, 2008. Dynamic Model for Power Systems with Multiple FACTS Controllers. Electric Power System Research, 78: 361-371.
38. Chu, C.C. and H.C. Tsai, 2008. Application of Lyapunov-Based Adaptive Neural Network Controllers for Transient Stability Enhancement. Power and Energy Society General Meeting, pp: 1-6.
39. Afzalian, A. and D.A. Linkens, 2000. Training of Neuro-Fuzzy Power System Stabilizers using Genetic Algorithms. International Journal of Electrical Power and Energy Systems, 22(2): 93-102.
40. Williams, R.J. and D. Zipser, 1989. A Learning Algorithm for Continually Running Fully Recurrent Neural Networks. Neural Computation, 1: 270-280.
41. Lin, F.J., P.H. Shen, S. Lin. Yang and P.H. Chou, 2006. Recurrent Radial Basis Function Network-Based Fuzzy Neural Network Control for Permanent-Magnet Linear Synchronous Motor Servo Drive. IEEE Transactions on Magnetics, 42(11): 3694-3705.
42. Juang, C.F. and C. D. Hsieha, 2010. Locally Recurrent Fuzzy Neural Network with Support Vector Regression for Dynamic-System Modeling. IEEE Transactions on Fuzzy Systems, 18(2): 261-273.
43. Lin, Y.Y., J.Y. Chang and C.T. Lin, 2013. Identification and Prediction of Dynamic Systems Using an Interactively Recurrent Self-Evolving Fuzzy Neural Network. IEEE Transactions on Neural Networks and Learning Systems, 24(2): 310-321.
44. Hingorani, N.G. and L. Gyugyi, 2000. Understanding FACTS: Concepts and Technology of Flexible AC Transmission Systems, New York: IEEE Press.
45. Sauer, P.W. and M.A. Pai, 2003. Power System Dynamics and Stability, Pearson Education, Singapore.
46. Mendel and M. Jerry, 2007. Uncertain Rule-Based Fuzzy Logic System: Introduction and New Directions. Edition 1, Prentice Hall, ISBN-10: 0130409693, ISBN-13: 978-0130409690.
47. Liu, Z., 2007. Self-tuning Control of Electric Machines using Gradient Descent Optimization. Optimal Control Application and Method, 28(2): 77-93.